A SAMPLE-COLLECTION DEVICE FOR SEM IMAGING AND ANALYSIS OF COKE DEPOSITS FROM LUBRICANT THERMAL DEGRADATION

A Thesis

by

NOBLE KNIGHT GUTIERREZ

Submitted to the Graduate and Professional School of
Texas A&M University
in partial fulfillment of the requirements for the degree of

MASTER OF SCIENCE

Chair of Committee,	Eric L. Petersen
Committee Members,	Chad Mashuga
	Adolfo Delgado
Head of Department,	Guillermo Aguilar

May 2023

Major Subject: Mechanical Engineering

ABSTRACT

Solid deposits form when a lubricant undergoes thermal breakdown due to high-temperature conditions and can cause adverse operational effects within engines. A collection device designed to allow coke to form on its surface was inserted inside of a test section to further study the physical characteristics of coke. The device was made from 0.003-inch-thick stainless steel 304 and went through several designs of varying cut-out shapes to form a test strip. The material of the coke-collecting test trip is the same as the test section. Three different lubricants were analyzed using a scanning electron microscope (SEM): a synthetic-blend motor oil (SAE 20W-50), a flushing/rust preventative oil, and Mobil DTE 732 which is a turbine oil. In each test, 400 mL of lubricant was circulated at 10.4 mL/min through a test section that is heated to 475 °C. Nitrogen was used to purge the system to study the effects of pyrolysis. The addition of the test strip into the test section was determined to not have a significant effect on the induction time when comparing two Mobil DTE 732 tests with and without the test strip. Two additional tests were conducted with motor oil at 445 °C to generate an Arrhenius plot of induction time. The elemental composition of each degraded oil was analyzed on the test strip using energy-dispersive spectroscopy (EDS). Differences in the microscopic structure of each oil was observed. The elemental composition for coke from turbine and motor oils was found to mostly consist of carbon, as expected. The usual additives of P, S, Ca, Zn, and Ba were found in the flushing/rust-preventative solid deposits. For the turbine deposits, the additives of P, Si, S, Ca, and Zn were identified. Lastly, for the synthetic-blend motor oil, additives of P, Mg, S, Ca, and Zn were detected.

ACKNOWLEDGMENTS

I would like to thank my committee chair, Dr. Petersen, for the opportunity, his enthusiasm and guidance throughout my work on the project. Dr. James Thomas' help was integral in obtaining data for this project and I thank him for his assistance. I would also like to thank Dr. Delgado and Dr. Mashuga for their service on my thesis committee.

Thanks also go to Mr. Carl Johnson at the TEES Turbomachinery Laboratory for his input in designing the shape of the test strip. I also thank Mr. Christian Landry for his help learning EDS software and Mr. Felix Rodriguez for recommending the SEM used in the project. Ms. Raquel Juárez Fúnez was fundamental in laying the ground-work for coking-rig experimental procedures and her guidance was invaluable for obtaining the data.

Finally, thanks to my parents for their encouragement and unwavering support throughout my life and work as a graduate student.

CONTRIBUTORS AND FUNDING SOURCES

Contributors

This work was supervised by a thesis committee consisting of Professors Eric Petersen and Adolfo Delgado of the Department of Mechanical Engineering and Professor Chad Mashuga of the Department of Chemical Engineering. Some data analyzed in Section 4 was provided by Ms. Raquel Juárez Fúnez.

All other work conducted for the thesis was completed by the student, under the advisement of Dr. Eric L. Petersen of the Department of Mechanical Engineering.

Funding Sources

Graduate study was supported by the Petersen research group within the TEES Turbomachinery Laboratory, and by the Texas A&M Engineering Experiment Station (TEES).

NOMENCLATURE

SEM	Scanning Electron Microscope
EDS	Energy-dispersive Spectroscopy
cps/eV	Counts per second per electron-volt

TABLE OF CONTENTS

Page

LIST OF FIGURES

Page

LIST OF TABLES

Page

1. INTRODUCTION

Extreme engine temperatures can severely degrade lubricating oils that produce carbonaceous deposits, known as coke, due to oxidative and thermal breakdown [1]. Coke deposits, shown in Figure 1, are black and mostly carbon that result from oxidation or thermal breakdown [1, 2]. These deposits are solid and interfere with reliable fluid flow, mechanical movements, increase wear rates, affect oil flow rates, damage seals, decrease heat transfer, and result in other issues. One of the oil degradation processes that contributes to coke formation happens via oxidation mainly when the oil's antioxidant package is depleted [3]. Other critical factors are the temperature the oil is exposed to and the time the oil is exposed to the hot temperatures. Reducing these two factors can decrease coke formation [4]. A lubricating oil has two main components which are a basestock and an additive package. About 72-96% of an engine oil is a basestock, and about 4-28% of the lubricant is composed of an additive package [5]. The base oil reduces friction, removes heat and wear particles, and separates moving surfaces by acting as a fluid layer while additives improve or create properties in the base oil.

The existing research available in the literature does not answer many questions with regards to lubricant degradation and even less so with SEM and elemental composition analysis of degraded oils. Since it is known that high operating temperature is a crucial factor in the degradation of an oil, it is desirable to understand what factors contribute to thermal breakdown without the factor of oxidation under pyrolysis. A rig

was developed for the purpose of degrading oil under controllable conditions called a coking rig [6-8]. There is a need for developing a method to non-destructively examine lubricant degradation under pyrolysis using such a rig.

Figure 1 Sample of coke deposits from coking rig.

In this thesis, the development of a coke-collection device is detailed and its results analyzed to further study lubricant degradation. Section 2 discusses the background information behind oil degradation and lubricant additives. Section 3 focuses on how the experimental apparatus works, the design of the coke-collection device, and the methods of data analysis. Finally, the results from the data collection are discussed in Section 4.

2. BACKGROUND

It is known that additives define the characteristics of a lubricant. It is of interest to identify the additives within different types of oils so that causation of degradation rates can be further analyzed. For motor oils, additives packages comprise 30% of the lubricant, whereas with turbine lubricants, additive packages make up around 1% of the oil [9]. Typical additives for lubricants include Mo, Mg, S, B, Ba, P, K, Ca, Zn, and Sb. Each element has a specific purpose for a specific application such as being corrosion inhibitors, rust inhibitors, detergents, dispersants, anti-wear additives, and antioxidants. Extremely high temperatures cause lubricants to degrade and can form into sludge, varnish, and solid deposits known as coke where each has unique physical characteristics [9-14]. Sludge is a muddy, messy substance, similar to grease, that can flow within a system and cause issues within valves and oil pathways by restricting oil flow. Varnish is a sticky substance that clings to surfaces but is not as messy as sludge. The higher the temperature of the system, the solid coke deposits that form become darker and more brittle. Thermal degradation compromises the lubricant's original attributes and shortens service life in addition to prematurely damaging lubricated gas turbine components, causing valves to stick, decreasing efficiency in cooling, and decreasing flow through or clog filters and small orifices [1, 15-18]. Solid deposit formations are great contributors to component failure in aircraft turbine engines and can result in catastrophic accidents [3, 19].

Arrhenius plots and the Arrhenius Rate Rule are used to rank lubricants based on oil degradation processes. According to a rule of thumb based on the Arrhenius Rate Rule, oxidation rates double for every 10°C increase in operating temperature [5, 13]. Just a 10°C change significantly impacts lubricant degradation. Arrhenius plots are convenient to show when an antioxidant package is depleted. The induction time is defined as the time it takes for coke to form [4]. The percentage of deposit formation is graphed versus time in Figure 2. A log scale is used to graph induction time versus the inverse of absolute temperature, as shown in Figure 3. Lubricants can be ranked according to temperature response and induction time using this technique. Higher temperatures with lower induction time lines demonstrate coke that was initiated faster, while lower temperature and higher induction time lines show that coke took longer to be produced.

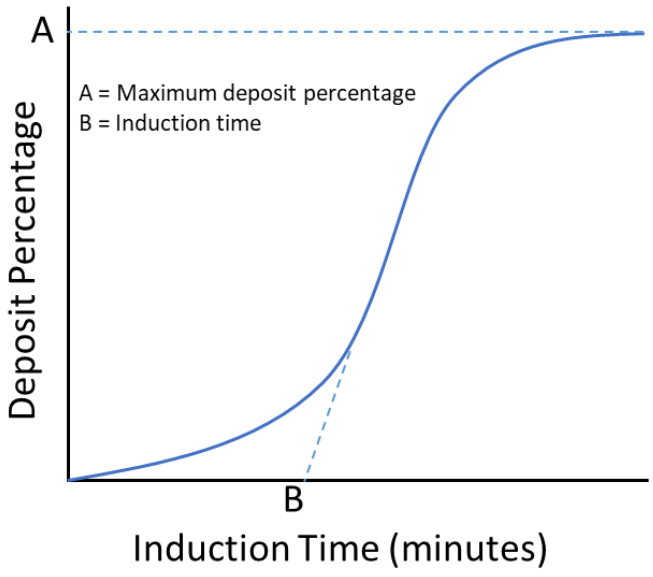

Figure 2 Arrhenius plot demonstrating that deposit percentage increases with time [6].

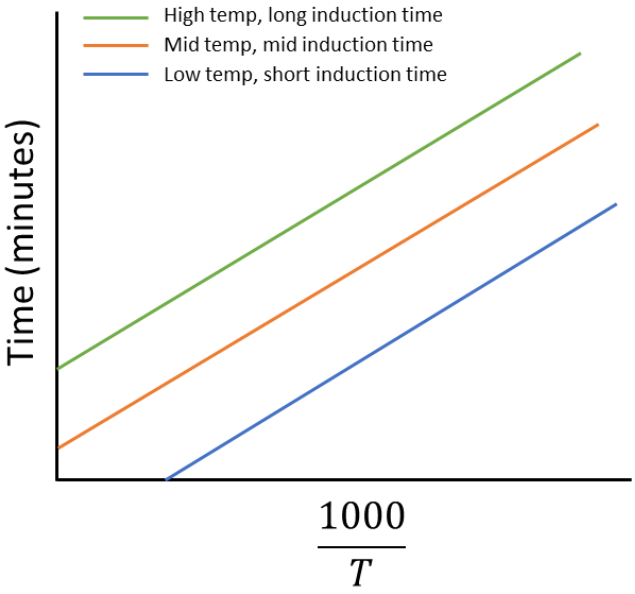

Figure 3 Arrhenius log scale plot displaying the rankings of different lubricants for certain temperatures and induction times [6].

3. METHODS AND DESIGN

3.1. Apparatus

A testing apparatus, referred to as a coking rig, was designed to analyze the effects of temperature on the coking induction time of oils as seen in Figure 2 [6-8, 20-22]. The oil circulates via a pump from Reservoir 1 through a test section that is heated by two band heaters that maintain a constant temperature over time. The oil then recirculates back into Reservoir 1. The oil flow rate can be adjusted by changing the frequency of the drive that controls the gear metering pump. The coking rig is pictured in Figures 4 and 5.

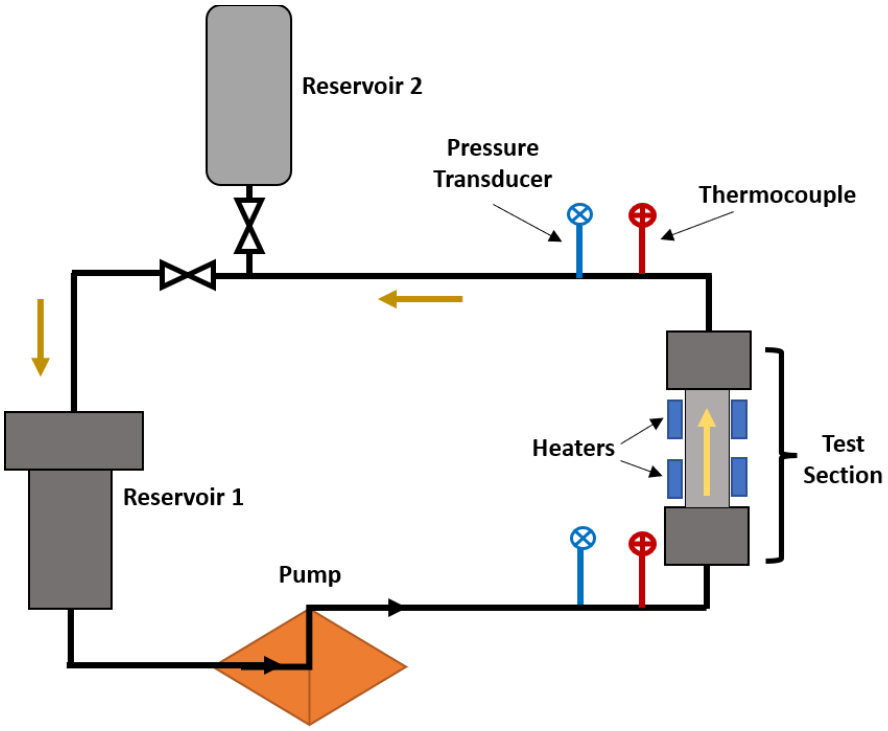

Figure 4 Schematic of experimental apparatus.

Figure 5 (a) Front of test rig and (b) back of test rig.

Since the effects of pyrolysis are desired to be investigated, the rig can be pressurized with nitrogen. The desired pressure can be maintained due to a pressure relief valve. As the oil degrades, coke forms on and sticks to the inner walls of the test section as seen in Figure 6. The coke deposits act as a barrier and reduce the heat transfer from the heaters to the oil, similar to the occurrences within an engine. As a result, the outlet temperature decreases as the oil reaches a lower temperature. The test section is made out of stainless steel 304 and has seven thermocouples that are embedded into the outer tube surface with a 0.05-inch gap from the inner tube surface, shown in Figure 7.

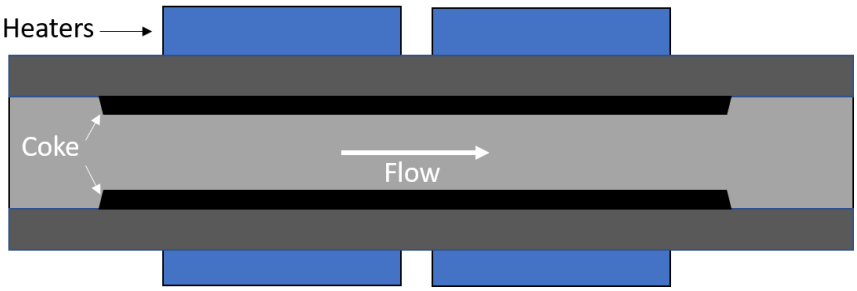

Figure 6 Cross-section of coking rig test section without test strip.

The thermocouples read the axial temperature distribution throughout the test section. The center thermocouple is connected to a temperature controller that maintains the set test temperature. Additionally, inlet and outlet thermocouples record the temperatures before and after the oil travels through the test section. All temperatures are recorded every 16 seconds in a computer-based data acquisition system. The test section can be seen with the thermocouples in Figure 8.

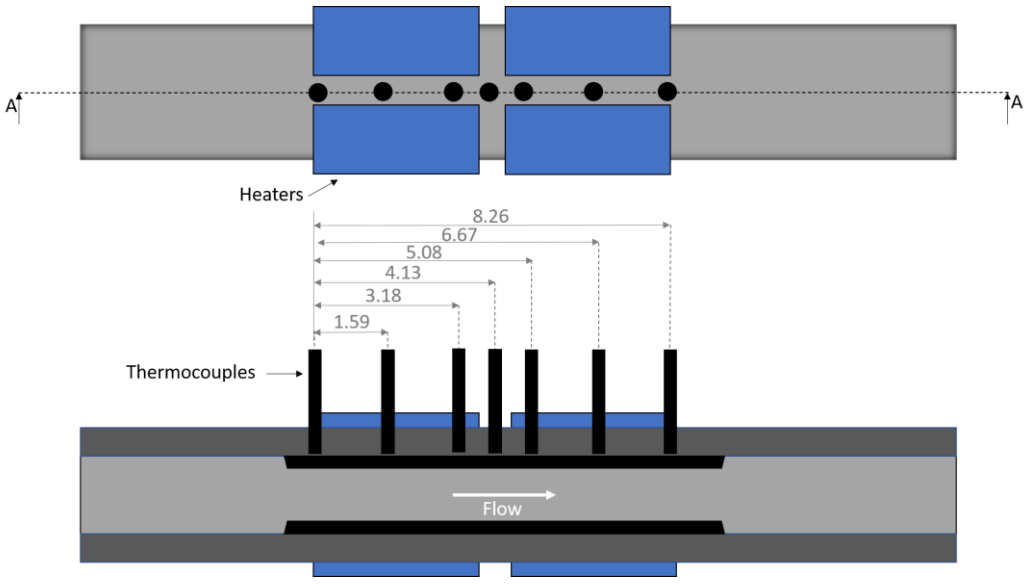

Figure 7 Cross-section of test section with thermocouples. Dimensions are in centimeters.

Figure 8 Test section with thermocouples.

3.2. Test Strip Design

A collection device was designed to allow coke to form on its surface within the test section to examine the coke more closely in a non-destructive manner. The device was made from 0.003-inch-thick stainless steel 304 and went through several designs of varying cut-out shapes using scissors to form a test strip. The material of the coke-collecting test trip is the same as the test section. Several iterations were required to obtain the desired amount of coke in a convenient fashion. The first iteration was conducted in an experiment with Mobil DTE 732 turbine oil and inserted in the test section as seen in Figure 9.

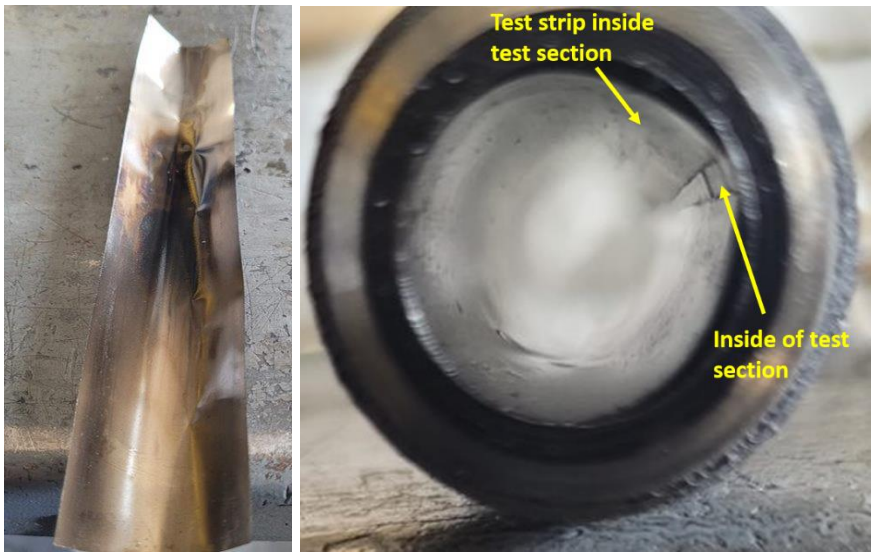

Figure 9 First iteration test strip.

The first iteration did not collect enough coke to be analyzed properly. A second iteration was needed and can be seen in Figure 10. This second design collected more coke on the surface of the test strip, however, the strip was not fully flush against the inner tube wall due to its thinner and weaker structure. Thus, a third design was needed that increased support in the center of the test strip so as to increase how flush it rests against the inner test section wall. Rib-like structures were added to the third iteration as seen in Figure 11. Nonetheless, a fourth and final design iteration, shown in Figure 12, was made for symmetrical purposes, and the dimensions were standardized for the rest of the tests involving the various oils.

Figure 10 Second iteration test strip.

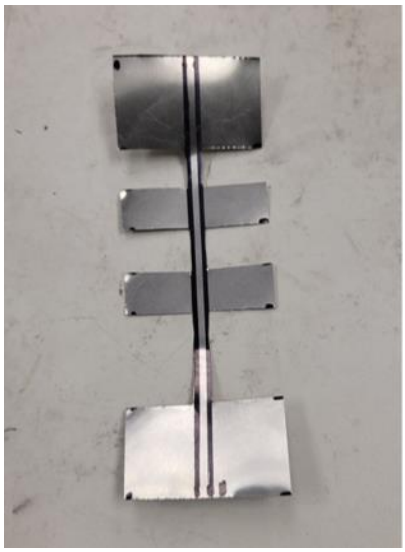

Figure 11 Third iteration test strip.

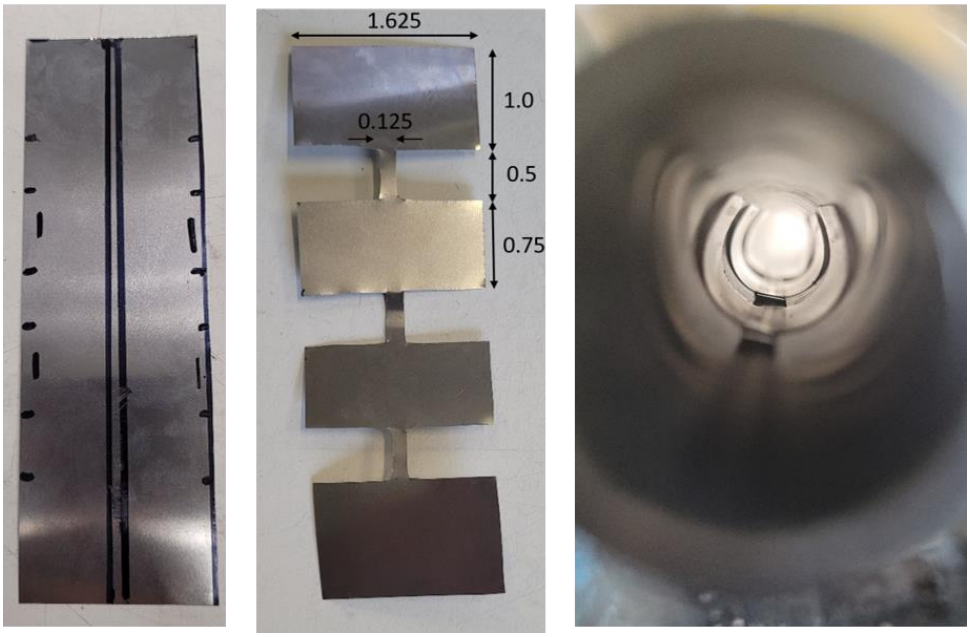

Figure 12 Final iteration of test strip. Dimensions are in inches.

The test strip was then removed from the test section at the end of every test and cut with scissors to isolate the region with coke on it and was inserted into a TESCAN VEGA3 SEM for further analysis [23]. Several regions of each coke sample were examined at different magnifications. The elemental composition of each region was mapped using EDS. The results of the SEM measurements are provided in the following section.

4. RESULTS AND DISCUSSION

4.1. Induction Time and Test Strip Results

4.1.1. Flushing/Rust-Preventative Oil

The results from the test strip with the flushing/rust preventative oil coke deposits can be seen in Figure 13. The oil generated a substantial layer of coke that formed on the strip. The corresponding temperature traces can be seen in Figure 14 where, in the red circle, there are sharp temperature changes that indicate the start of coke formation.

Figure 13 Flushing/rust preventative oil test strip with coke.

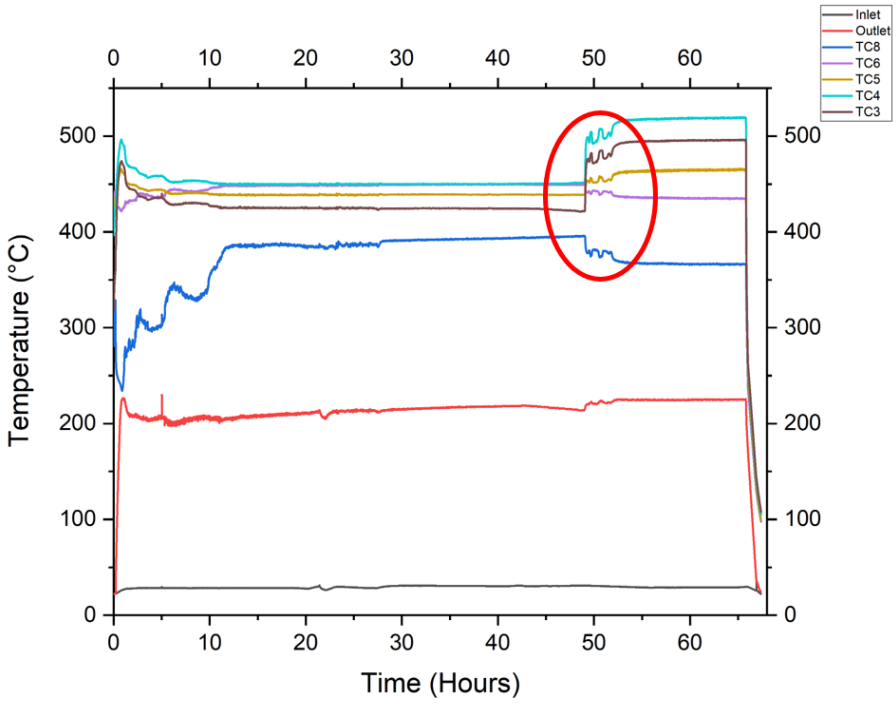

Figure 14 Flushing/rust preventative oil and surface temperatures recorded from test section, inlet, and outlet. The test was conducted with the central thermocouple set to 475 °C with a flow of 10.4 mL/min for around 65 hours.

4.1.2. Mobil DTE 732

The results from the test strip with Mobil DTE 732 turbine oil coke is pictured in Figure 15. The test strip was cut so as to isolate the region with the most coke to be inserted into the SEM. The full oil and surface temperatures recorded from test section, inlet, and outlet can be seen in Appendix A. The corresponding induction time graph can be seen in Figure 16.

Figure 15 Mobil DTE 732 test strip with coke.

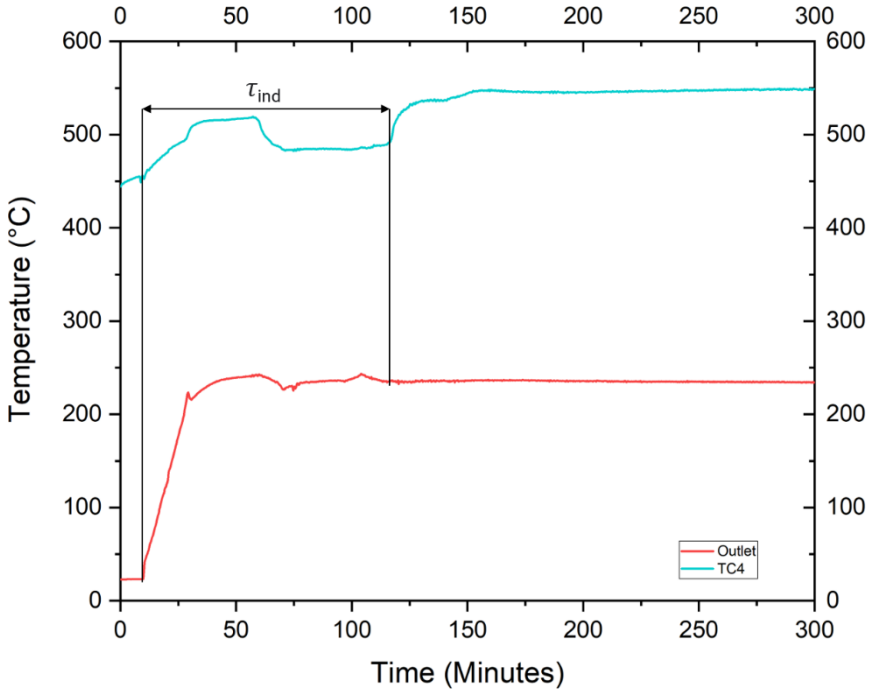

Figure 16 Mobil DTE 732 induction time with test strip for a test completed using 400 mL of oil flowing at 10.4 mL/min with the central thermocouple set to 475 °C.

To see if the test strip affects the induction time, Figure 16 can be compared with the induction time graph of a test run under the same oil and conditions but without the test strip, shown in Figure 17. The induction times for each test can be seen in Table 1. The induction times were within 11 minutes of each other, which is reasonable and it can be accepted that the test strip does not have a significant effect on the induction time.

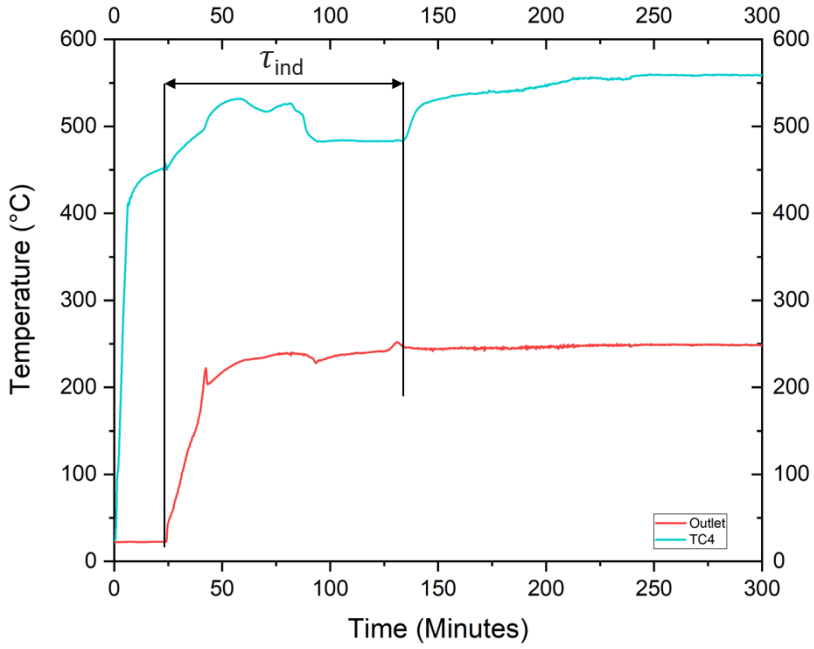

Figure 17 Mobil DTE 732 induction time without test strip for a test completed using 400 mL of oil flowing at 10.4 mL/min with the central thermocouple set to 475 °C.

Table 1 Induction time for Mobil DTE 732 with and without the test strip.

Induction time with test strip	98 min
Induction time without test strip	109 min

4.1.3. Motor Oil

Three individual experiments were run with SAE 20W-50 motor oil at 475 °C. Two representative motor oil coke samples can be seen in Figure 18. The temperature traces from one of the experiments is shown in Figure 19. Additional tests were run with the same motor oil at 445 °C to create an Arrhenius plot of induction time. Both lower-temperature tests are shown in Figures 20 and 21. The lower-temperature tests had fewer visible results with regards to seeing sharp temperature changes usually seen when coke forms at the higher-temeprature tests. When the test strip was taken out after the lower-temperature tests, there was a lot more sludge than coke compared to the higher-temperature experiments.

Figure 18 Two samples of SAE 20W-50 motor oil test strips with coke from 475 °C run.

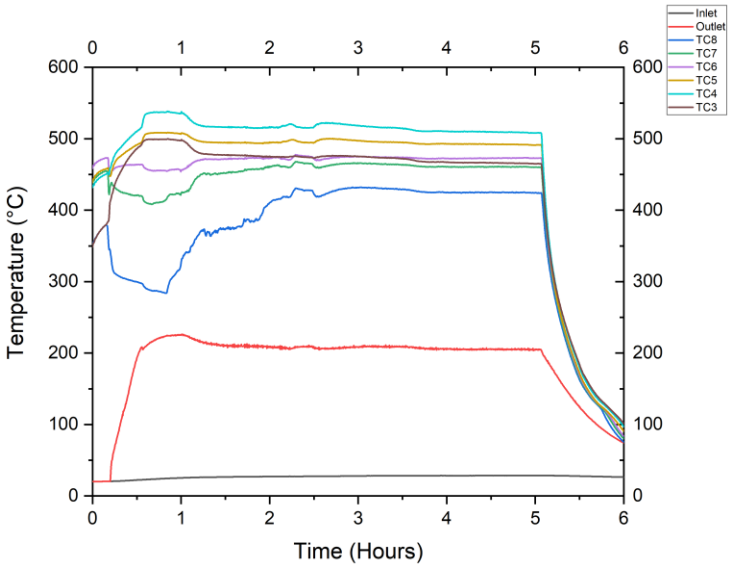

Figure 19 One of three higher-temperature tests with SAE 20W-50 motor oil. The test was conducted with the central thermocouple set to 475 °C with a flow of 10.4 mL/min for around 5 hours.

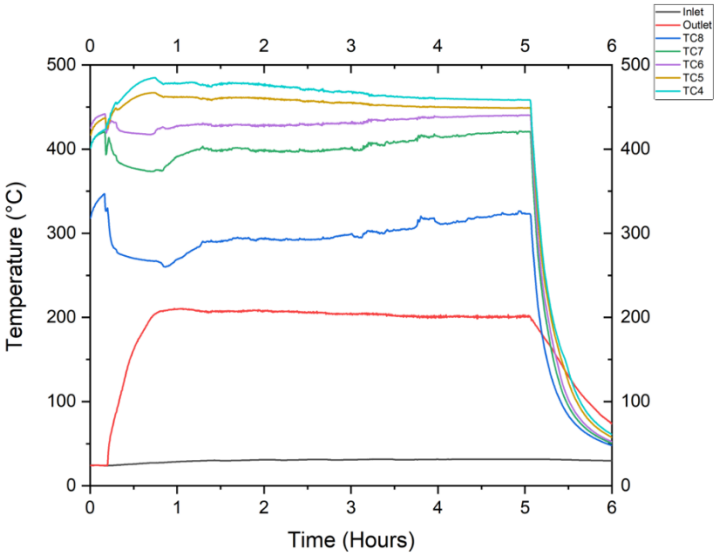

Figure 20 One of two lower-temperature tests with SAE 20W-50 motor oil. The test was conducted with the central thermocouple set to 445 °C with a flow of 10.4 mL/min for around 5 hours.

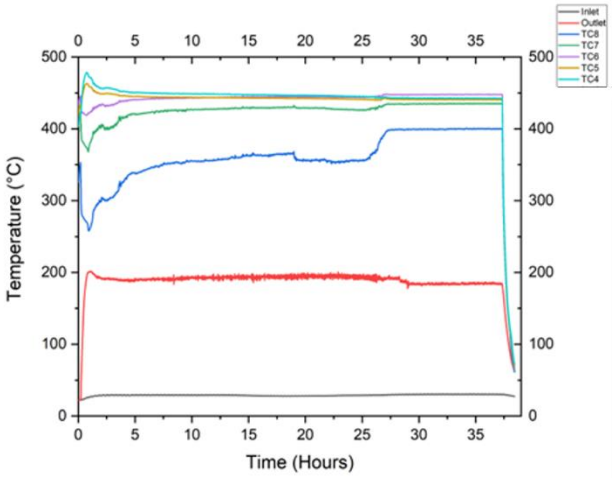

Figure 21 Second of two lower-temperature tests with SAE 20W-50 motor oil. The test was conducted with the central thermocouple set to 445 °C with a flow of 10.4 mL/min for around 40 hours.

The induction times for the three higher temperature tests as well as the induction times for the two lower-temperature tests are listed in Table 2. The induction times for experiments 1-3 are within 16 minutes of each other. The induction times for experiments 4-5 are within 13 minutes of each other and are around 60-90 minutes longer than the higher-temperature runs. The Arrhenius plots for both temperatures are shown in Figure 22.

Table 2 Induction time for SAE 20W-50 motor oil at 445 °C and 475 °C.

Experiment 1 induction time at 475 °C	122 min
Experiment 2 induction time at 475 °C	126 min
Experiment 3 induction time at 475 °C	138 min
Experiment 4 induction time at 445 °C	212 min
Experiment 5 induction time at 445 °C	199 min

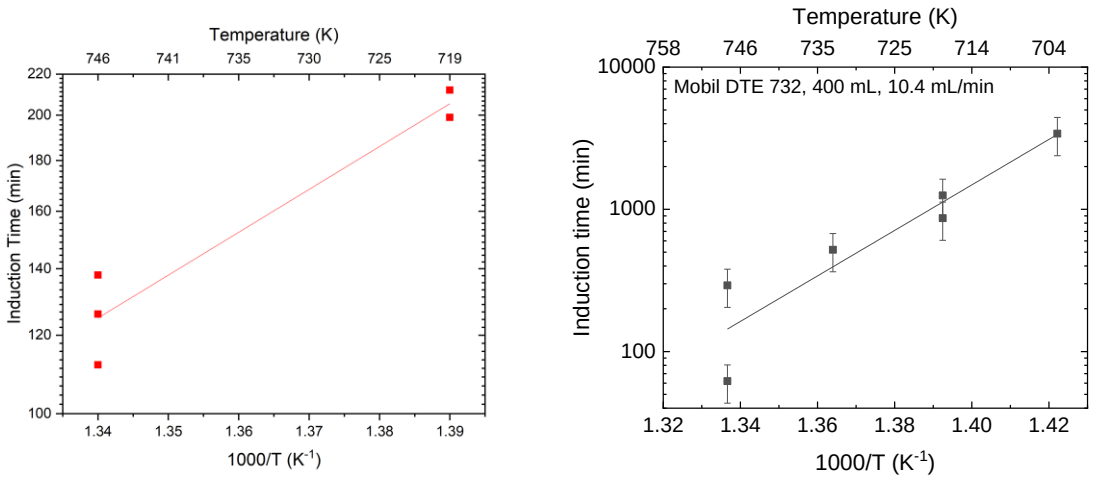

(a) (b)

Figure 22 Measured induction time on an Arrhenius plot for (a) SAE 20W-50 motor oil at set temperatures of 445 °C and 475 °C and (b) Mobil DTE 732 of varying temperatures from 430 °C to 475 °C [20].

4.2. SEM and EDS Results

4.2.1. Flushing/Rust-Preventative Oil

Two regions of the coke sample from the flushing/rust-preventative oil were analyzed, and the SEM and EDS results for one of these regions are shown in Figure 23. The different elements are color coded for visual inspection. A high concentration of carbon is seen in red and is the majority of the elemental composition. Higher quality images of the structures within the coke are captured from the SEM in Figure 24.

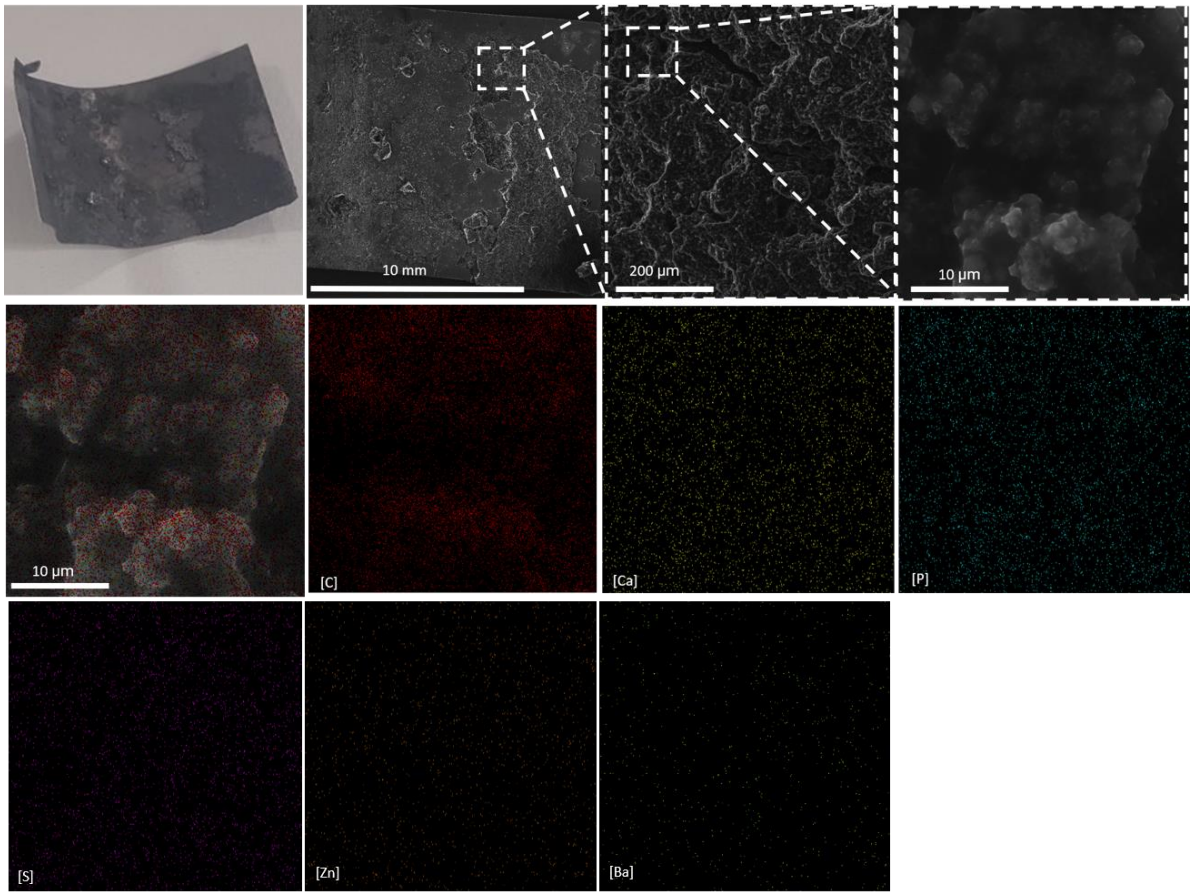

Figure 23 Region 1 SEM images of flushing/rust-preventative oil coke with corresponding EDS mapping analyses for visualization of elemental dispersion.

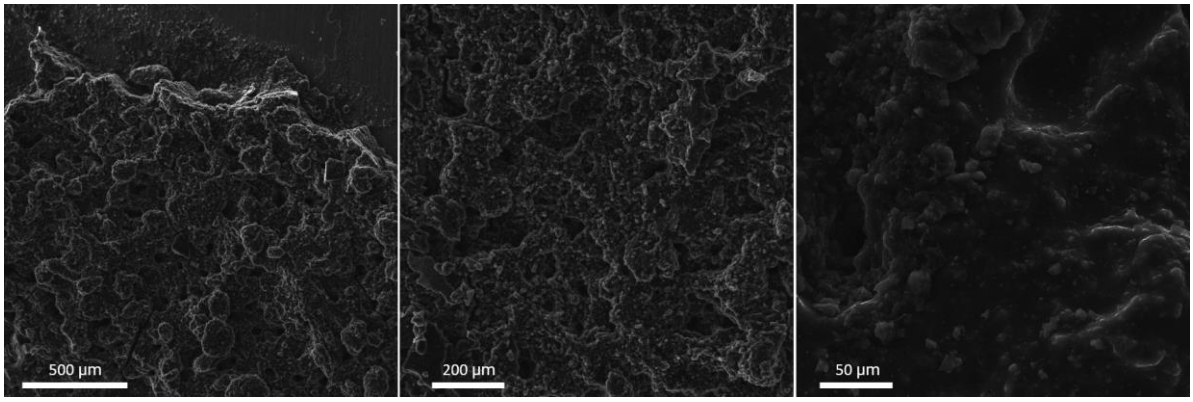

Figure 24 Various SEM images of coke from flushing/rust-preventative oil.

The coke spectra from the EDS software along with the percent weight for each element for both regions of the same sample are graphed in Figure 25. The elemental percent weight is based on analyzing each pixel of the particular region during EDS. The EDS mapping can be found for the second region in Appendix A. The percent weight and percent weight sigma values are tabulated in Appendix B. The percent weight sigma values are statistical error values for the calculated percent weight from the EDS software. It is important to note that since the test strip is made of stainless steel 304, some of that metal can appear in the EDS results. Stainless steel 304 is made of 18% Cr, 8% Ni, 2% Mn, 0.10% N, 0.03% S, 0.08% C, 0.75% Si, and 0.045% P [24].

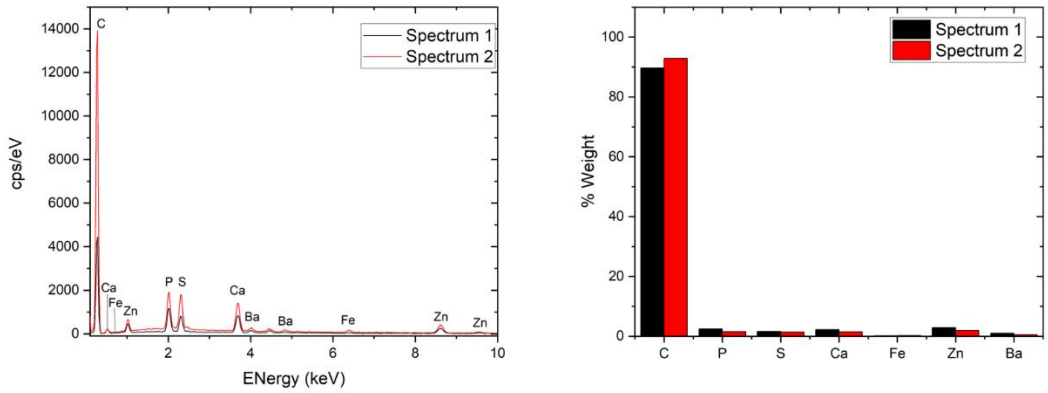

Figure 25 Flushing/rust preventative oil coke spectra and elemental weights from regions 1 and 2.

4.2.2. Mobil DTE 732

Three regions of the coke sample from the Mobil DTE 732 turbine oil were analyzed, and the SEM and EDS results for one of these regions are shown in Figure 26. It is interesting to see that Fe and Ca are captured at the edges surrounding the larger

coke region in addition to the normal elements found in stainless steel 304. A high concentration of carbon is seen in red and is the majority of the elemental composition as with the previous oil. Interesting, bubble-like structures and other features within the coke are captured from the SEM in Figure 27.

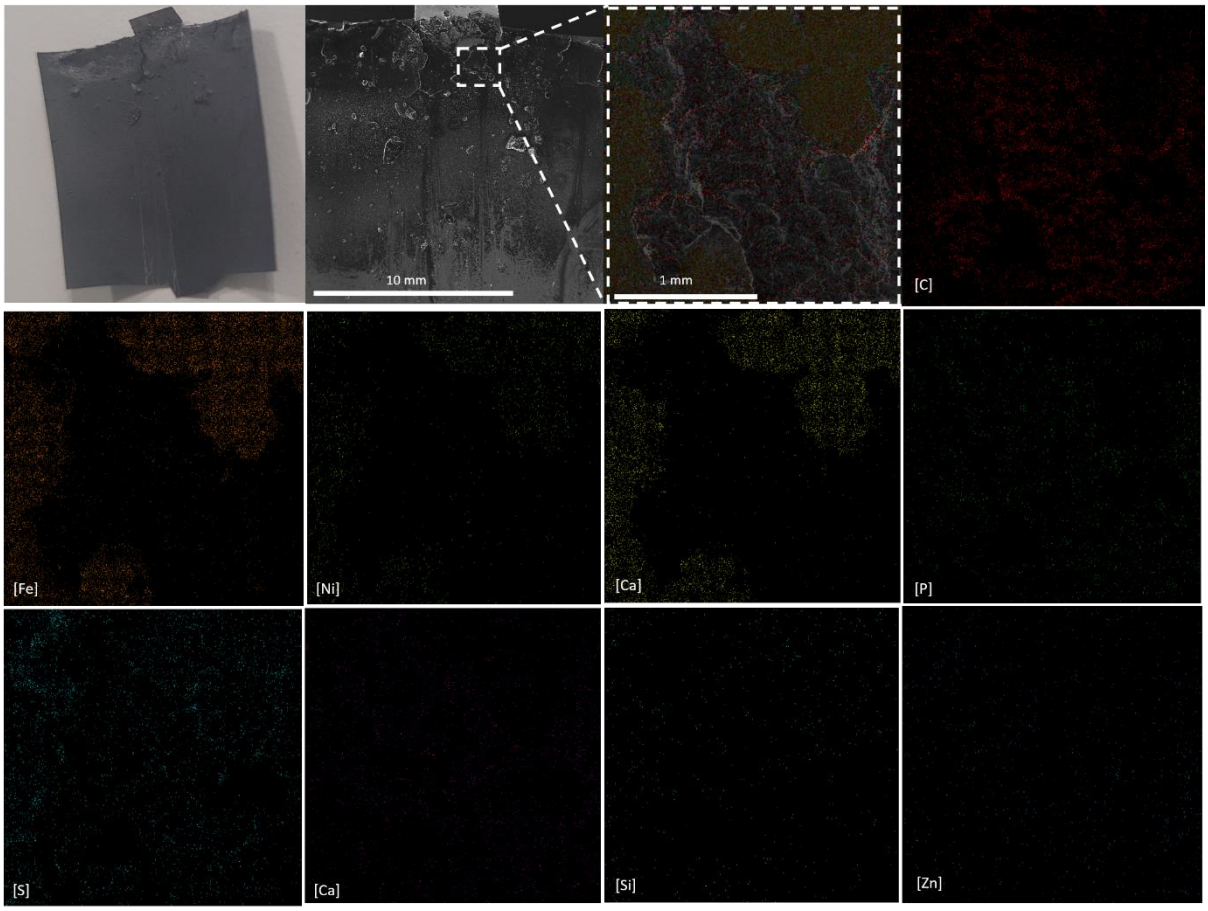

Figure 26 Region 1 SEM images of Mobil DTE 732 coke with corresponding EDS mapping analyses for visualization of elemental dispersion.

EDS results for regions 2 and 3 can be seen in Appendix A. The coke spectra from the EDS software along with the percent weight for each element for regions 1-3 of the same sample are graphed in Figure 28. It is notable that Zinc was detected in one of

the analyzed regions of the solid deposit sample as Mobil DTE 732 it is claimed to be a Zinc-free oil. This detection could possibly be from the coking rig system to be slightly contaminated from previous tests with other oils. The percent weights for all three regions are tabulated along with corresponding percent weight sigma values in Appendix B.

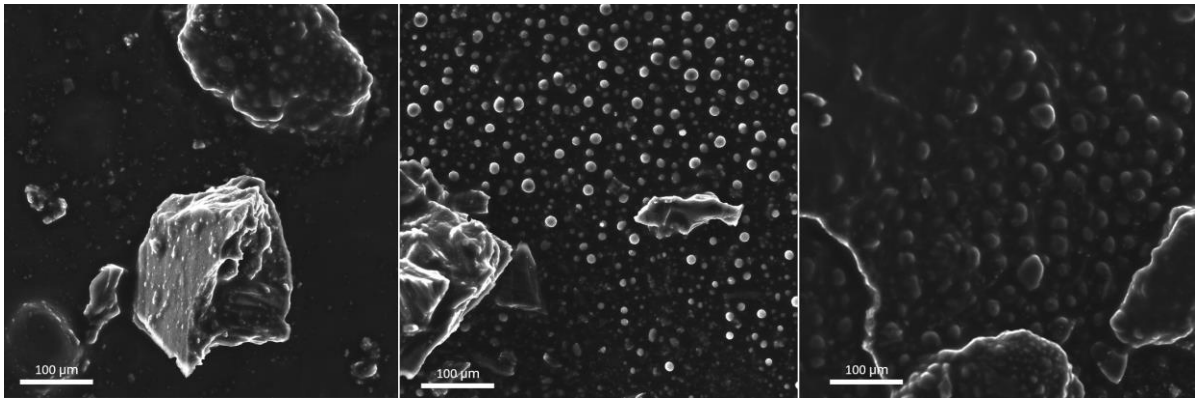

Figure 27 Various SEM images of coke from Mobil DTE 732.

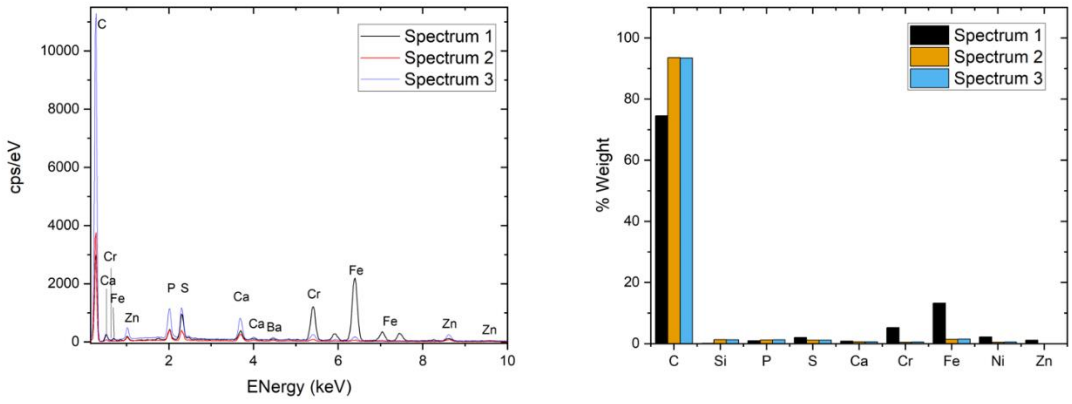

Figure 28 Mobil DTE coke spectra and elemental weights from regions 1-3.

4.2.3. Motor Oil

All three samples of the coke from the motor oil were analyzed, and the SEM and EDS results for one of the samples are shown in Figure 29. As with both previous oils, a high concentration of carbon is seen in red and is the majority of the elemental composition. Interesting, crater-like structures within the coke are captured from the SEM in Figure 30.

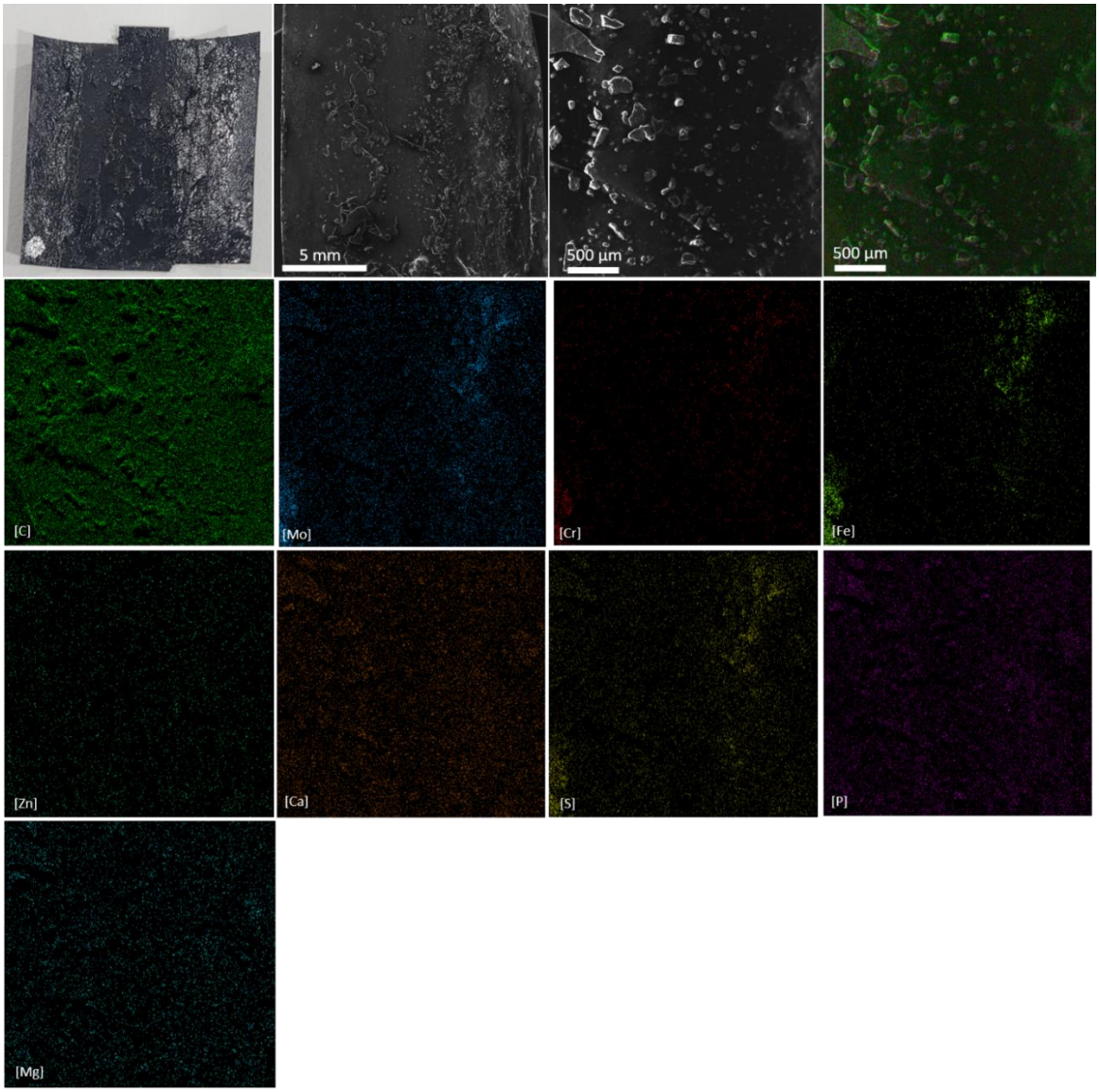

Figure 29 One of three sample SEM images of SAE 20W-50 motor oil coke with corresponding EDS mapping analyses for visualization of elemental dispersion.

EDS results for experiments 2-3 of the same oil can be seen in Appendix A. The coke spectra from the EDS software along with the percent weight for each element for experiments 1-3 of the same oil are graphed in Figure 31. Additional elements were detected in the motor oils such as oxygen, aluminum, and magnesium. The percent weights for all three experiments are tabulated along with corresponding percent weight sigma values in Appendix B. The detected element of aluminum is significantly lower in percent weight and has a relatively higher percent weight sigma value that makes it negligible.

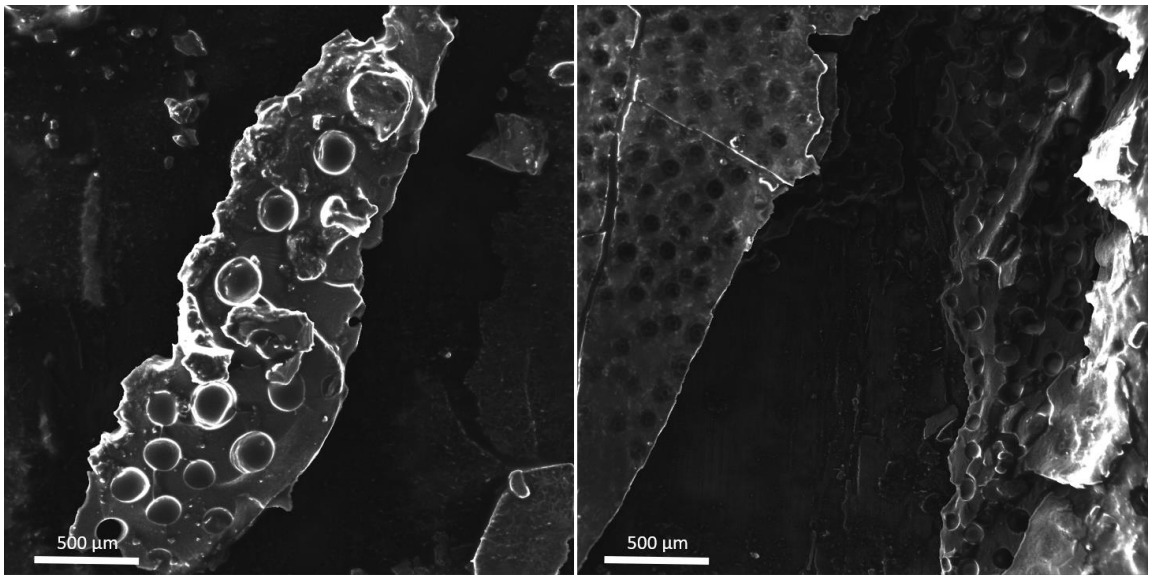

Figure 30 Experiment 2 motor oil coke SEM images.

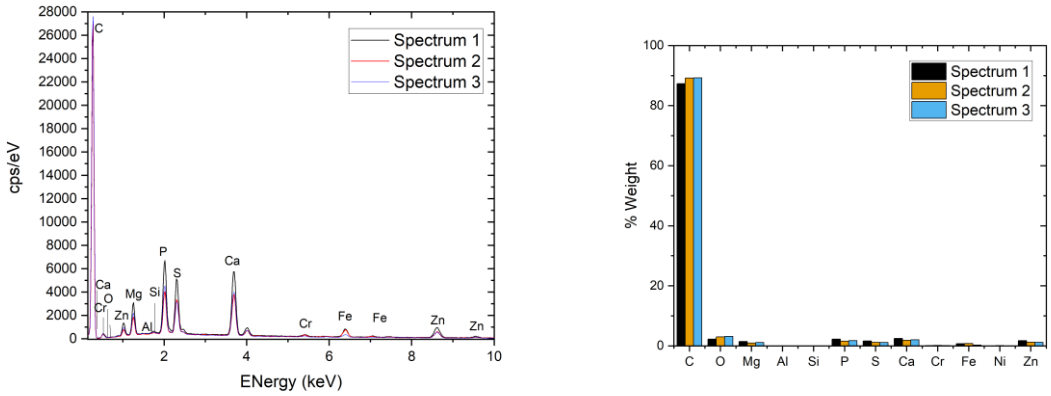

Figure 31 Motor oil coke spectra and elemental weights from experiments 1-3.

5. CONCLUSIONS

5.1. Summary

A new coke-collection device was designed and developed to allow solid deposits to form on its surface for non-destructive analysis. The test strip was inserted into the test section of a coking rig where oil is run to degrade oil. Three different lubricants were analyzed using a scanning electron microscope (SEM): a synthetic-blend motor oil (SAE 20W-50), a flushing/rust-preventative oil, and Mobil DTE 732 which is a turbine oil. In each test, 400 mL of lubricant was circulated at 10.4 mL/min through a test section that is heated to 475 °C. Nitrogen was used to purge the system to study the effects of pyrolysis. After each test, the test strip was taken out of the test section and cut to isolate the region with coke to be non-destructively analyzed with an SEM.

The addition of the test strip into the test section was determined to not have a significant effect on the induction time when comparing two Mobil DTE 732 tests with and without the test strip. Two additional tests were conducted with motor oil at 445 °C to generate an Arrhenius plot of induction time which was comparable to the spread of a turbine oil however with much lower induction time. The elemental composition of each degraded oil was analyzed on the test strip using energy-dispersive spectroscopy (EDS).

Differences in the microscopic structure of each oil was observed, and bubble-like structures were identified in Mobil DTE 732 coke, whereas crater-like structures were found in the motor oil deposits. The elemental composition for coke from turbine and motor oils was found to mostly consist of carbon, as expected. Additives of P, S,

Ca, Zn, and Ba were found in the flushing/rust-preventative solid deposits. For the turbine deposits, the additives of P, Si, S, Ca, and Zn were identified. Lastly, for the synthetic-blend motor oil, additives of P, Mg, S, Ca, and Zn were detected.

5.2. Recommendations

With further testing and analysis, explanations can be explored as to what causes the different structures found in coke deposits such as with the bubble-like and crater-like structures. Examining the additives and percent weight at different conditions and times in the process of coke formation would be of interest such as identifying elemental composition of the oil before degradation and after varying durations of tests or temperatures with the same oil. Using air to pressurize the system instead of nitrogen to view the effects of oxidation would also be a possibility.

REFERENCES

[1] Exxon Mobil Corporation, "Tech Topic: Coking", 2016.

[2] Edge, R. G., and Squires, A. T. B. P., "Lubricant Evaluation and Systems Design for Aircraft Gas Turbine Engines," *SAE Technical Paper*, No. 690424, 1969. https://doi.org/10.4271/690424

[3] Kauffman, R. E., Feng, A. S., and Karasek, K. R., "Coke Formation from Aircraft Turbine Engine Oils: Part I — Deposit Analysis and Development of Laboratory Oil Coking Test," *Tribology Transactions*, Vol. 43, No. 4, 2000, pp. 823-829. https://doi.org/10.1080/10402000008982414

[4] Kauffman, R., Feng, A., and Karasek, K., "Coke Formation from Aircraft Engine Oils: Part II—Effects of Oil Formulation and Surface Composition," Tribology Transactions, vol. 43, no. 4, pp. 677-680, 2000. Available: 10.1080/10402000008982395.

[5] Pawlak, Z., Tribochemistry of Lubricating Oils. Amsterdam: Elsevier, 2003.

[6] Gutierrez, Noble Knight (2021). Pyrolysis and Solid Deposit Formation of Lubrication Oils. Undergraduate Research Scholars Program. Available electronically from https : / /hdl .handle .net /1969 .1 /194324.

[7] Juárez, R., Gutierrez, N., and Petersen, E. L., "Characterization of an Apparatus to Study Solid Deposit Formation in Lubricating Oils at High Temperatures," *Journal of Turbomachinery*, Vol. 145, No. 3, 2022. https://doi.org/10.1115/1.4055650

[8] Juárez, R., Gutierrez, N., and Petersen, E. L., "High-Temperature Degradation and Coking of Aircraft Gas Turbine Engine Lubricants," AIAA SCITECH 2023 Forum, 2023. https://doi.org/10.2514/6.2023-1252

[9] Mathura, S. (2020). Lubrication Degradation Mechanisms: A Complete Guide (1st ed.). CRC Press. https://doi-org.srv-proxy2.library.tamu.edu/10.1201/9781003102274

[10] Santos, J., Santos, I., and Souza, A., "Thermal Degradation Process of Synthetic Lubricating Oils: Part I—Spectroscopic Study", Petroleum Science and Technology, vol. 33, no. 11, pp. 1238-1245, 2015. Available: 10.1080/10916466.2015.1047031.

[11] Martynov, V., and Morozova, M., "Thermal Stability of Lubricants", Khimiya i Tekhnologiya i Masel, vol. 1, no. 11, pp. 46-50, 1965. Available: 10.1007/bf00719195.

[12] Livingstone, G., Thompson, B., and Okazaki, M., "Physical, Performance, and Chemical Changes in Turbine Oils from Oxidation", Journal of ASTM International, vol. 4, no. 1, p. 100465, 2007. Available: 10.1520/jai100465.

[13] Fitch, J., and Gebarin, S., "Review of Degradation Mechanisms Leading to Sludge and Varnish in Modern Turbine Oil Formulations," Journal of ASTM International, vol. 3, no. 8, 2006. Available: 10.1520/jai13504.

[14] Diaby, M., Sablier, M., Le Negrate, A., El Fassi, M., and Bocquet, J., “Understanding Carbonaceous Deposit Formation Resulting from Engine Oil Degradation”, Carbon, vol. 47, no. 2, pp. 355-366, 2009. Available: 10.1016/j.carbon.2008.10.014.

[15] Gschwender, L. J., Snyder, C. E., Nelson, L., Fultz, G. W., and Saba, C. S., "Advanced High-Temperature Air Force Turbine Engine Oil Program," *Turbine Lubrication in the 21st Century*, ASTM International, West Conshohocken, PA, 2001, pp. 17-24.
[16] Novotny-Farkas, F., Baumann, K., and Leimeter, T., "Optimizing the Thermo-Oxidation Stability of Gas Turbine Oils," *Goriva i Maziva*, Vol. 47, No. 3, 2008, pp. 220-231.
[17] Rowland, R. G., Dong, J., and Migdal, C. A., "Antioxidants," *Lubricant Additives: Chemistry and Applications*, 3rd ed., CRC Press, Boca Raton, FL, 2017.
[18] Bardasz, E. A., and Lamb, G. D., "Additives for Crankcase Lubricant Applications," *Lubricant Additives: Chemistry and Applications*, 3rd ed., CRC Press, Taylor & Francis Group, Boca Raton, FL, 2017, pp. 457-491.
[19] Wu, N., Zong, Z.-M., Fei, Y.-W., and Ma, J., "Studies on Thermal Oxidation Stability of Aviation Lubricating Oils," *MATEC Web of Conferences*, Vol. 114, 2017, p. 02002. https://doi.org/10.1051/matecconf/201711402002
[20] Juarez, Raquel; Petersen, Eric L. (2022). "Coking of Gas Turbine Lubrication Oils at Elevated Temperatures." Turbomachinery Laboratory, Texas A&M Engineering Experiment Station. Available electronically from https : / /hdl .handle .net /1969 .1 /197035.
[21] Petersen, Eric & Mathieu, Olivier & Thomas, James & Cooper, Sean & Teitge, David & Juarez, Raquel & Gutierrez, Noble & Mashuga, Chad. (2021). Combustion and Oxidation of Lube Oils at Gas Turbine Conditions: Experimental Methods. 10.1115/GT2021-60319.
[22] Juarez, R., Gutierrez, N. and Petersen, E. L., 2021, "Pyrolysis of Motor Oil in Contact With High-Temperature Surfaces Leading to Solid Deposit Formation," Proceedings of the 12th U.S. National Combustion Meeting, College Station, TX, May 24-26.
[23] Texas A & M University; Texas; USA (RRID: SCR_022128)
[24] Lenntech, "Stainless Steel 304."

APPENDIX A

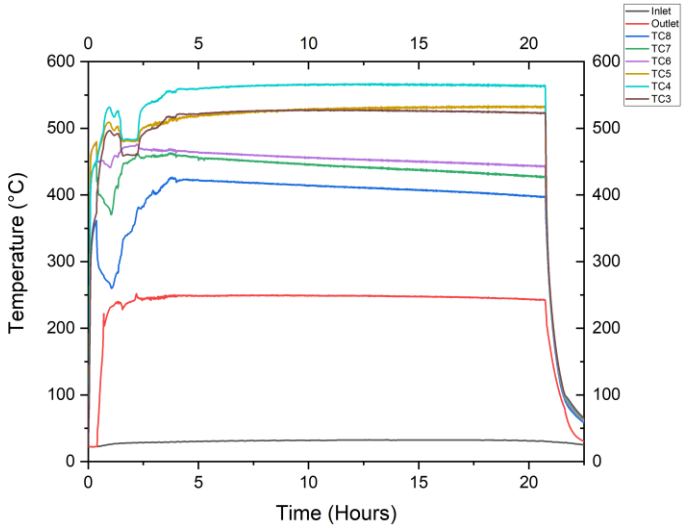

Figure 32 Mobil DTE 732 oil and surface temperatures recorded from test section, inlet, and outlet without test strip. The test was conducted with the central thermocouple set to 475 °C with a flow of 10.4 mL/min for around 20 hours.

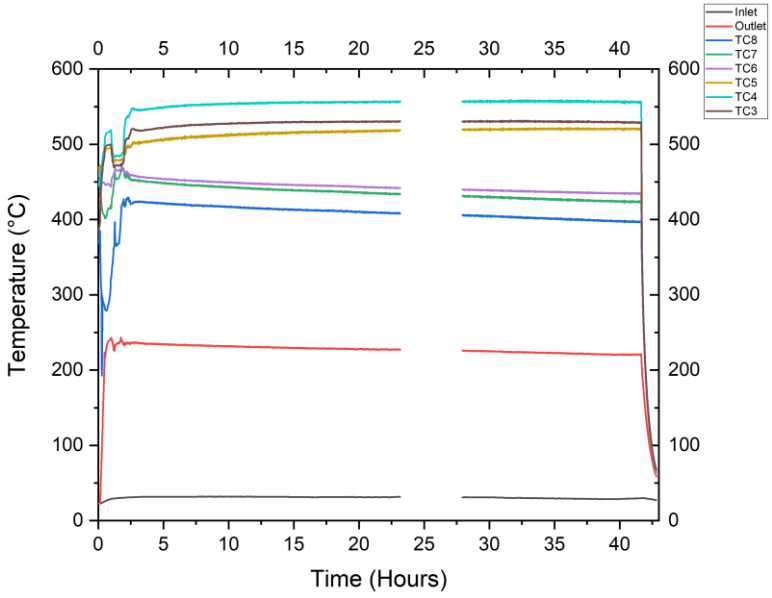

Figure 33 Mobil DTE 732 oil and surface temperatures recorded from test section, inlet, and outlet. The test was conducted with the central thermocouple set to 475 °C with a flow of 10.4 mL/min for around 40 hours.

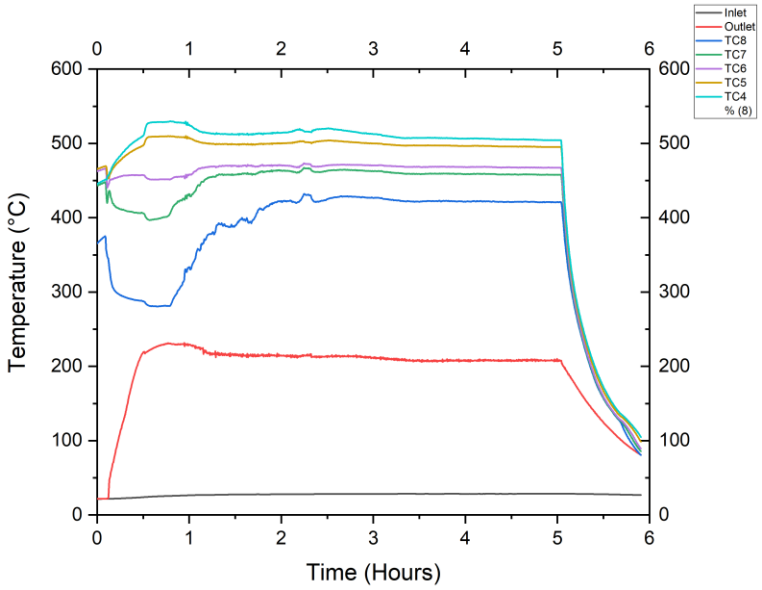

Figure 34 Second of three SAE 20W-50 motor oil and surface temperatures recorded from test section, inlet, and outlet. The test was conducted with the central thermocouple set to 475 °C with a flow of 10.4 mL/min for around 5 hours.

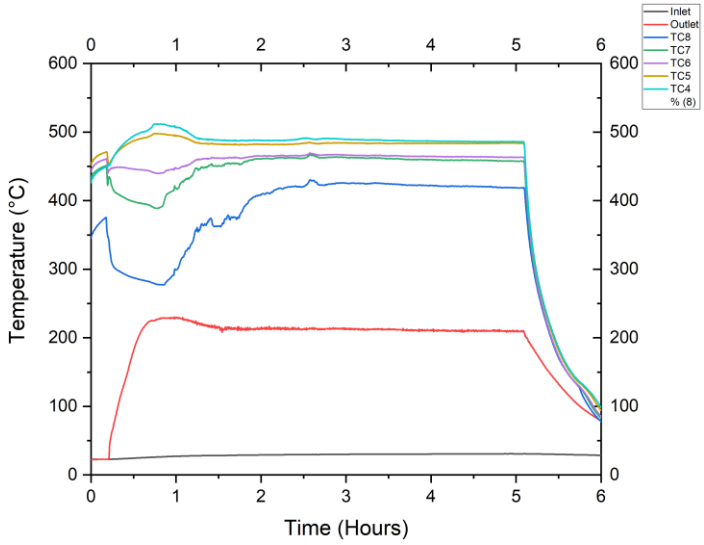

Figure 35 Third of three SAE 20W-50 motor oil and surface temperatures recorded from test section, inlet, and outlet. The test was conducted with the central thermocouple set to 475 °C with a flow of 10.4 mL/min for around 5 hours.

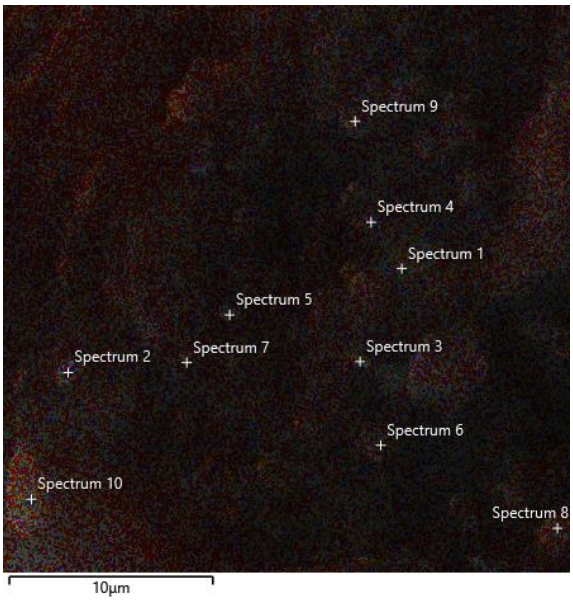

Figure 36 Flushing/rust preventative oil coke layered EDS region 2.

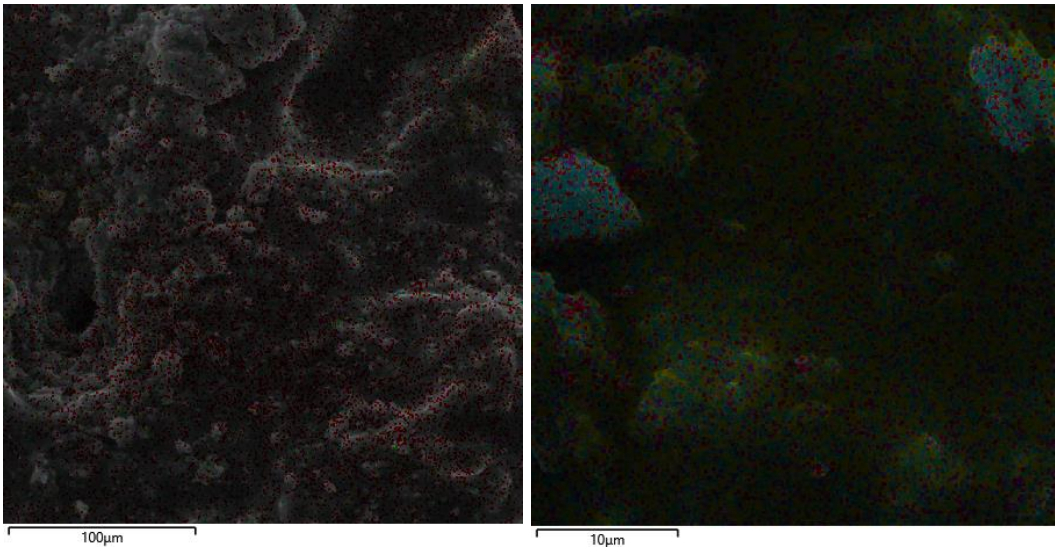

Figure 37 Mobil DTE 732 coke layered EDS region 2 (left) and region 3 (right).

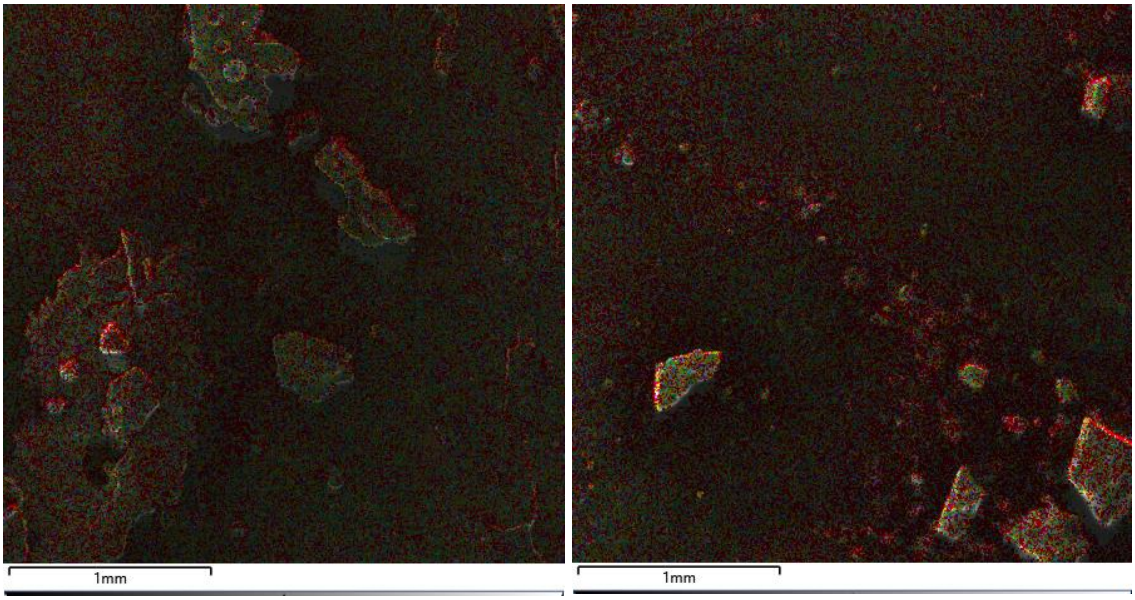

Figure 38 SAE 20W-50 motor oil coke layered EDS region from two separate experiments.

APPENDIX B

Table 3 Flushing/rust-preventative oil coke % weight and sigma values for regions 1 and 2.

	Spectrum 1		Spectrum 2	
Map Sum Spectrum	% Weight	% Weight Sigma	% Weight	% Weight Sigma
C	89.7	0.21	92.88	0.11
P	2.47	0.07	1.53	0.04
S	1.63	0.06	1.39	0.03
Ca	2.24	0.06	1.45	0.03
Fe	0.14	0.04	0.26	0.03
Zn	2.87	0.12	1.92	0.06
Ba	0.96	0.09	0.57	0.05
Total	100	-	100	-

Table 4 Mobil DTE 732 coke % weight and sigma values for regions 1-3.

	Region 1		Region 2		Region 3	
Map Sum Spectrum	% Weight	% Weight Sigma	% Weight	% Weight Sigma	% Weight	% Weight Sigma
C	74.52	0.39	93.58	0.2	93.43	0.12
Si	0.13	0.03	1.29	0.06	1.24	0.04
P	0.9	0.05	1.18	0.06	1.21	0.03
S	1.98	0.06	1.12	0.06	1.1	0.03
Ca	0.78	0.04	0.55	0.06	0.56	0.03
Cr	5.23	0.12	0.44	0.06	0.49	0.03
Fe	13.21	0.23	1.43	0.11	1.49	0.06
Ni	2.16	0.09	0.42	0.09	0.49	0.05
Zn	1.1	0.1	0	-	0	-
Total	100	-	100	-	100	-

Table 5 Motor oil coke % weight and sigma values for experiments 1-3.

	Experiment 1		Experiment 2		Experiment 3	
Map Sum Spectrum	% Weight	% Weight Sigma	% Weight	% Weight Sigma	% Weight	% Weight Sigma
C	87.3	0.19	89.16	0.21	89.26	0.21
O	2.25	0.18	2.98	0.21	3.16	0.21
Mg	1.44	0.03	0.96	0.03	1.12	0.03
Al	0	0.01	0.02	0.01	0.01	0.01
Si	0.06	0.01	0.04	0.01	0.05	0.01
P	2.24	0.03	1.56	0.02	1.75	0.03
S	1.63	0.02	1.2	0.02	1.13	0.02
Ca	2.47	0.03	1.86	0.02	2.01	0.03
Cr	0.11	0.01	0.16	0.02	0.08	0.01
Fe	0.7	0.02	0.75	0.02	0.28	0.02
Ni	0.07	0.02	0.08	0.02	-	-
Zn	1.72	0.04	1.23	0.04	1.16	0.04
Total	100	-	100	-	100	-